

Answer to reviewer 2

This document is the list of our responses to the reviewer's comments and a revised version of the text is also attached to this response to show the changes in red and the deleted sentences using strikethrough text

Summary: DIAL Ozone profiles and IAGOS in situ data are presented during the 2022 ACROSS campaign on 21 days. These profiles are compared to the the satellite observations of Infrared Atmospheric Sounding Interferometer (IASI). Ancillary measurements from microlidar and radiosondes are also used for contextualizing the dynamics of the atmosphere. To better understand the regional transport of polluted air masses advected over the city, daily ozone analysis of the Copernicus Atmospheric Service (CAMS) ensemble model 10 and on backward trajectories of the Paris city plume were also utilized.

Major Comments: This paper aims to discuss the importance of DIAL profiles on understanding the pollution transport on several high ozone days during ACROSS 2022. This effort is unfortunately not very well documented or referenced and reads closer to a campaign report, rather than a scientifically significant manuscript.

We warmly thank the reviewer for his/her suggestions and comments.

In the introduction the objectives of the paper have been presented more explicitly with the following paragraph:

“The presentation of the O₃ vertical observations available during this period as well as a preliminary analysis of the respective contribution of the urban boundary layer structure and of the O₃ plume regional transport are the main objectives of this paper. The latter has been extensively discussed for North American campaigns listed hereabove, but it is not clear if similar conclusions can be drawn for the Paris area about the role of elevated ozone concentrations transported from outside the megacity area. The Paris area is also different from the places with complicated pollution plume recirculation due to orography or land-sea breeze meteorological forcing where many previous campaigns took place in Europe or North America. Therefore it is relevant to present a study specific to the development of ozone pollution episode in the Paris area.

The overall description of the O₃ variability during the ACROSS campaign and the selection of the pollution events analyzed in this work are presented in section 3.1. This section focusses on lidar observations and their comparison with aircraft and model data. The comparison of the ACROSS O₃ vertical profiles and satellite observations, as well as a comparison of the pollution events in term of regional O₃ transport and PBL dynamical development are discussed in section 4. Section 4.1 first shows to what extent the O₃ measurements discussed in this work are relevant for studying the summer day-to-day variability of ozone in the lower troposphere in Paris, including the potential input from satellite observations. Section 4.2 presents the analysis of the regional O₃ transport during ACROSS since this process has been recognized during the past campaigns as a significant source of variability. Sections 4.3 and 4.4 summarize the main characteristics of the summer pollution episodes encountered during ACROSS and put the results into a broader perspective by comparing them with those of past measurement campaigns”

The structure of the paper has been modified to make the contribution of the work more readable with firstly a section 3 presenting the measurements discussed in the paper with fewer figures and more synthetic and with secondly a section 4 discussing the analysis of the results. We have modified figures 5 to 12 (now figures 5 to 7) and have moved the microlidar data presentation in the supplementary document to focus on the ozone data analysis as requested by reviewer 1. A

summary table (Table 3) has been added to present the main characteristics of the summer pollution episodes encountered in Paris during ACROSS in section 4.3 and this section has been expanded to present the 3 main findings derived from this work. A new subsection 4.4 is added discussing similarities and differences with results obtained during past campaigns. A careful copy editing of English writing has been made.

We agree that the level of detail in the presentation of the different measurement days makes difficult to emphasize the summary section 4. However, as in the numerous papers describing measurement campaigns, including those listed by the reviewer, it remains important to provide the reader with the information needed to contextualize the observations. We did our best to balance section 3 and 4 to show that the paper goes beyond a campaign report.

Section 4 has been expanded to summarize the main findings and add a new summary table (Table 3). The new version of section 4.3 now includes the following text:

“Table 3 summarizes the main characteristics of the summer pollution episodes encountered in Paris. The diversity of long range transport and its role in O₃ variability means that this table can be considered sufficiently representative of the conditions that lead to a summer O₃ increase in a city like Paris. Three main conclusions can be drawn from our analysis:

- Westward advection of the pollution plume from continental Europe enhance the O₃ increase over the city of Paris. The contribution of an increase in O₃ background has already been widely demonstrated for other megacities in North America, such as deep stratospheric intrusions or forest fire plumes (see next section). Deep stratospheric intrusions are rare from May to September in North Western Europe in comparison with North America (Akritidis et al., 2021). Long range transport of forest fire plumes are also detected in Europe, but at higher altitude (>5km) than in North America (Baars et al., 2021) with less contribution to the low troposphere O₃ background. Therefore westward advection of the pollution plume from continental Europe is a significant contribution for the Paris area.

- High temperatures in Paris are often accompanied by a southerly flow carrying Saharan dust in the 2-5 km altitude range over northern France (Israelevich et al., 2012). This study show that the downward entrainment of the low O₃ plume at the top of the polluted PBL must be accounted for to understand a possible mitigation of the PBL ozone increase during a summer heat wave.

- The maximum altitudes of the O₃ plume change from 1.5 km up to 3 km. The capability of IR satellite observations can be assessed using the ACROSS O₃ profile observations. Our study shows that IASI 0-3 km tropospheric O₃ column is sensitive to the day-to-day O₃ variability in the lower troposphere, especially when using the AM IASI observations. The significant underestimate of the 0-3 km partial column when the O₃ plume remains below 1.5 km, is reduced as soon as the plume maximum altitude exceeds 2 km.”

There is mention of pollution and ozone precursors, but the authors have failed to pull in any sort of additional chemical observations besides ozone. CAMS or IAGOS NO_x or other species will help bolster the conclusions of pollution transport or why there are potentially differences between the measurements.

The reviewer is right saying that there is no ozone precursor measurement included in this work. We tried to include the ACROSS ATR42 aircraft data in the paper, but there were not available for the days with elevated ozone pollution presented in this paper, except on June 22nd. However for this day the interesting feature is an ozone plume forming above 1.5 km, while the ATR42 flew at low level below 500 m (see Fig. R1 only included in this answer). The NO_x plume observed by the ATR42 west of Paris below 500 m is consistent with the CAMS NO₂ simulation now shown in Fig. 10 west of Paris. We therefore choose to rely mainly on CAMS simulations to characterize the formation and transport of the ozone plume at the regional scale. This is also

why we say in the introduction and conclusion that it is a preliminary study of the ozone pollution events encountered during ACROSS and that additional data set and modelling dedicated to the ACROSS analysis must be considered in a future work.

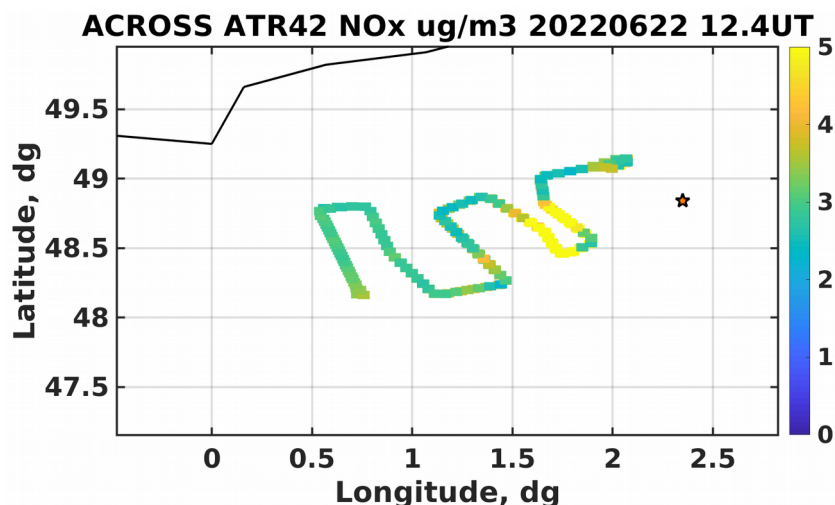


Fig. R1: ATR42 aircraft measurement of NO_x in ug/m³ horizontal distribution on June 22 from 12-14 UT at 400 m

In addition to the CAMS O₃ simulations presented in section 3, a new figure (Fig. 10) is added to show the CAMS NO₂ plumes distributions on June 16-17 and June 21-22 to strengthen the discussion about the regional plume transport in section 4.2. The purpose of this figure is to show the consequence of the June 16-17 advection of the Saharan plume and the June 21-22 advection of the Continental European plume on the NO₂ distribution and therefore the ozone photochemical production.

The following text is added then in section 4.2:

“The NO₂ plume CAMS simulations (Fig.10) also show the advection of the low O₃ streamer located over Brittany and the English Channel on June 16 and east of Paris on June 17. The low O₃ layer measured by the DIAL above 1.5 km in Paris is indeed a regional feature not specific to the Paris city center.”

“This is consistent with an aerosol plume of European continental pollution observed by the SLIM lidar on June 21 (Fig.S5a) and the advection of NO₂ continental plume and corresponding high O₃ concentrations from eastern to western France on June 22 (Fig.10). The low NO₂ concentrations east of the city center in the CAMS simulation (Fig.10) also explain the positive differences observed on June 22 between the city center DIAL and the IAGOS in-situ observations (Fig.7) when the aircraft was flying east of Paris (Fig S2)”

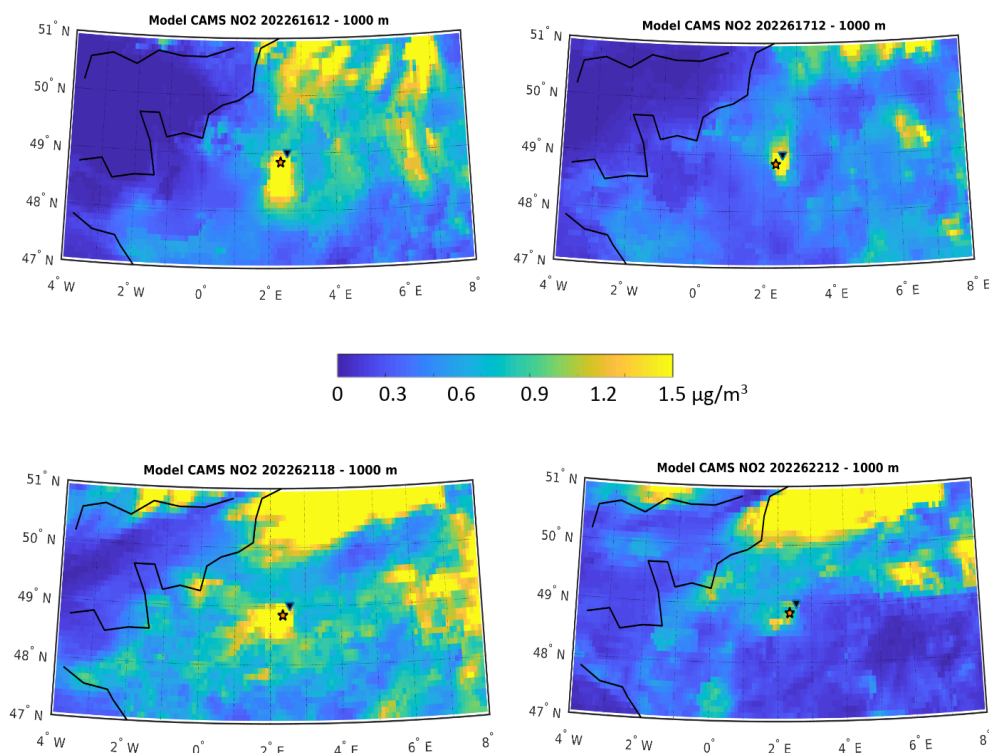


Fig. 10: CAMS ensemble mean NO₂ at 1000 m above Northern France on June 16 and 17 (top row) when dust plume advection at the PBL top is observed by the aerosol lidar and on June 21 and 22 (bottom row) when continental aerosol and O₃ plume advection at the PBL top is observed by both lidar. The orange star and dark-blue triangle are respectively the DIAL position and the CDG airport. The color scale is NO₂ concentration in $\mu\text{g}\cdot\text{m}^{-3}$.

Furthermore, the IASI measurements are not carefully assessed, some work needs to be done in understanding the inherent value and uncertainty of these measurements.

In the revised manuscript, we have applied the IASI observational operator to the IAGOS, LIDAR and CAMS data. We have changed Figure 13 (new figure 8), to show both the raw and smoothed IAGOS, LIDAR and CAMS data. Finally, we have also modified Table 2 to directly compare raw and smoothed values of O₃ partial columns between IASI and the other observed/modeled data. The text of section 4.1 has been completely changed to discuss the new figure and Table. See also answer to reviewer 1 for more details.

Comments below are intended to help the paper form a more thorough conclusion.

Minor Comments: There is a lack of appropriate and topical references throughout most of the manuscript. References to previous air quality/ozone campaigns should be refreshed for more recent work, in addition to expanding to other megacities.

We fully agree that the first version of the paper did not sufficiently detail the contribution of the numerous past campaigns, e.g. the results obtained in North America since the setup of the TOLNET network. We apologize for not having been explicit enough on this point, even if the previous introduction already recalled the numerous existing contributions on the role of processes controlling the intensity of pollution episodes. The introduction has been updated with the following text:

“Several campaigns took place in North America to characterize high O₃ summer concentrations: Texas Air Quality Study (TexAQs) 2000 and 2006 and TRacking Aerosol

Convection Experiment - Air Quality (TRACER-AQ) 2021 in Southwestern USA (Daum 2004, Senff 2010, Liu 2023), California Research at the Nexus of Air Quality and Climate Change (CalNex), California Baseline Ozone Transport Study (CABOTS) 2016, Las Vegas Ozone Study (LVOS) 2016 and 2017 in California (Ryerson 2013, Langford 2022, Faloon 2020), Long Island Sound Tropospheric Ozone Study (LISTOS) 2018 and 2019 in New York City (Couillard 2021). During these campaigns extensive use of aircraft and lidar were conducted to better understand the sources and formation mechanism of O₃ plumes (Langford 2019). Results of LISTOS, CABOTS and TRACER-AQ show that meteorology and boundary layer heights are significant parameters influencing the vertical distribution of O₃ in these areas. Sullivan (2017) demonstrated that residual O₃ layer reincorporation with mixed layer development contributes to a significant part of surface O₃ concentration increase in the afternoon. Contribution of long range transport of O₃ has been also analyzed using airborne differential absorption LIDAR (DIAL) and satellite. For example it was shown that regional transport of O₃ from Asian emissions over the North Pacific Ocean to California is responsible for a significant part of lower tropospheric O₃ increase in Summer (Lin 2012, Langford 2017) and that stratospheric-tropospheric exchanges (STE), forest fires and Asian pollution significantly control baseline ozone and therefore O₃ pollution in urban area in North America (Langford 2022, Wang 2021, Faloon 2020)."

A new section 4.4 is now devoted to comparing ACROSS results with those of previous campaigns, in particular those with the TOLNET network:

"LISTOS 2018-2019 and Southwestern USA campaigns took place in places and time periods which can be best compared with ACROSS, i.e. with limited fire and intercontinental pollution and STE. The main difference with LISTOS is the lack of land-sea breeze recirculation for Paris. Ozone concentrations exceeded 200 µg.m⁻³ during LISTOS with stagnation and land-sea breeze recirculation not seen during ACROSS (Couillard et al., 2021). The regional advection of European continental O₃ plume and of Saharan dust outbreak frequently associated to heat wave and pollution episode are also specific of the Paris area. Regarding the comparison with the TEXAQS and TRACER-AQ Southeastern USA campaigns, large O₃ concentrations > 200 µg.m⁻³ are observed near Houston due to the contribution of numerous petrochemical plants in addition to the city emissions (Parrish et al., 2009; Senff et al., 2010), while such O₃ concentrations have never been reached during ACROSS. The same conclusion can be drawn from the comparison with the ESCOMPTE campaign O₃ observations when petrochemical plant and ship emission contributions to O₃ plume formation are comparable to the Houston area (Drobniski et al., 2007). The O₃ long range transport observed during the Southwestern USA campaigns (CABOTS, LVOS) is different from the conditions encountered during ACROSS since STE, fire emission and Asian pollution plume transport significantly contributed to the O₃ inflow upstream of the local emission sources especially at altitudes above 2 km (Langford et al., 2022, 2017; Faloon et al., 2020). The latter makes difficult a direct comparison with the level of O₃ pollution encountered during ACROSS. The main similarity with the ACROSS results is the good agreement between the wide extension of the O₃ streamers shown by both the chemical transport models and the lidar and aircraft observations (Langford et al., 2022; Zhang et al., 2020). Indeed the CAMS model analysis during ACROSS are consistent with the O₃ observations presented in this paper and also show that the role of easterly flow from continental Europe replaces that played by the long range transport of fires and Asian pollution plumes during the Southwestern USA campaigns."

L90 – Reference needed as to where this statement can be drawn from “The accuracy of the lidar observations is altitude-dependent being of the order of 7µg.m⁻³ below 1000 m and occasionally increases up to 20 µg.m⁻³ above 2 km at midday”. Also recommend adding in a percentage difference. Please also note somewhere the conversion to ppbv for these observations - 1 ppb O₃ = 1.96 µg/m³ at 25°C and 1 atm

Done

Fig. 3 – Higher resolution terrain maps in the background would help better understand the ozone transport throughout the time. Adding in the wind barbs would also contextualize which direction the plume was moving.

We did not include terrain map as orography is not an issue for studying the Paris area. We cannot easily produce a wind representation corresponding to the CAMS simulations in Fig. 3 and 4. These two figures with multiple panels contain already a lot of information and there is a dedicated section (section 4.2) dedicated to the analysis of the regional transport based on FLEXPART simulations

Fig 6b – Is the CBLH actually over 3.5-3.8km? This seems unrealistic, even with >30°C temperatures. Is this an aged polluted air mass that has recirculated associated with the synoptic high pressure system over the area as mentioned in the text. This figure should be clarified or manual inspection of the CBLH algorithm should be addressed. How did CAMS compare in terms of the RL and CBLH observations?

We agree that June 18 is an unusual event of CBLH growth over Paris, especially considering the time of the CBLH maximum (20:30 UT). All the CBLH calculations shown in this paper have been manually checked. We are also confident with this value as the radiosounding inversion layer was also at 3.5 km at 20 UT on this day. Also surface temperature was 38 °C on this day (Fig. 2). We anyway do not want to focus our paper too much on this interesting case in terms of PBL dynamical development because O₃ DIAL observations after 15 UT are not available and O₃ was decreasing at the surface on June 18th because of the pollution mitigation by the dust plume advection over Northern France.

Fig 9 – It's unclear where and when these IAGOS data overlap. For instance on 20220615, what is the coincidence in time for the CAMS (or IAGOS) and DIAL?

The direct comparison between IAGOS, CAMS and DIAL vertical profiles is now better shown in the new section 3 (Fig. 7). We keep only the days where the comparison of IAGOS and DIAL is meaningful using daily mean and we take into account only the lidar data that can be best compared with IAGOS (measurement times are now included in Fig. 7). On June 15 there is a single IAGOS flight at 14 UT while the DIAL data are missing from 10-15 UT, therefore the comparison with IAGOS is not considered anymore in Fig. 7.

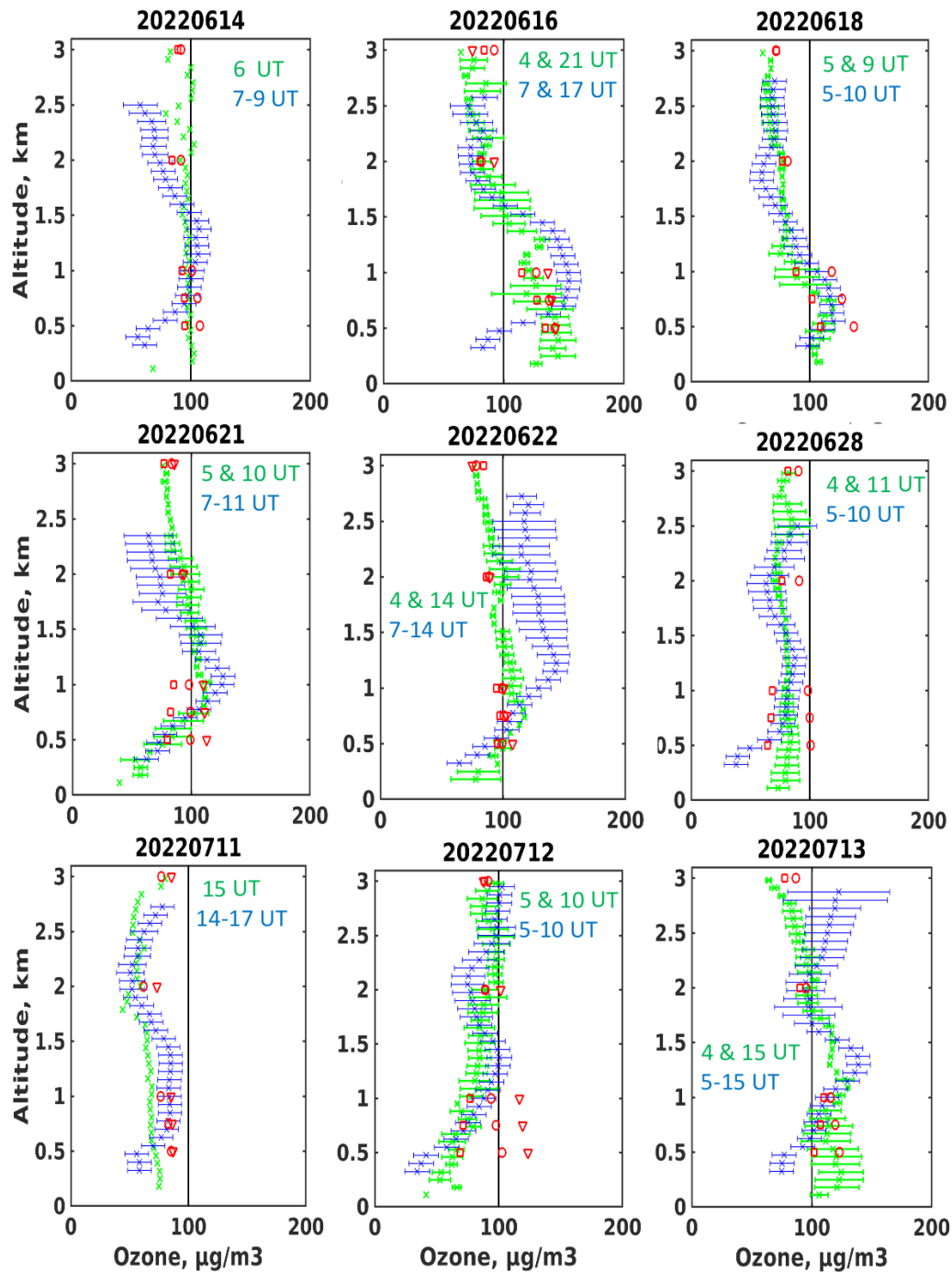


Figure 7. Daily mean O_3 vertical profiles in $\mu g \cdot m^{-3}$ for the IAGOS aircraft (green) and the corresponding DIAL observations (blue) shown in Fig.5 to 6. Green times in UTC labeled within the figures are the IAGOS measurement times above Paris (two profiles per day except on June 14 and July 11). Blue times below the IAGOS flight times show the selection of the DIAL observations. CAMS model vertical profiles are also shown using horizontal averages of the model concentrations included in the Fig.1 area. CAMS profiles are shown at 6 UT (red \square), 12 UT (red \circ) and 18 UT (red ∇).

Table 2 – are the \pm associated with the variance of the dataset or uncertainty associated with the observations? The relative levels of uncertainty between high precision DIAL and in-situ observations needs to be described in comparison to the likely much higher uncertainty satellite observations.

The \pm reflects the 1-sigma standard deviation around the mean for all dataset, not the uncertainties. In the revised manuscript, we have applied the IASI observational operators to the

IAGOS, LIDAR and CAMS data in order to take into account the differing characteristics of the observing systems, particularly their averaging kernels and error covariances of the satellite observations (Rodgers and Connor, 2003). We have also modified Table 2 to directly compare raw and smoothed values of O₃ partial columns between IASI and the other observed/modeled data.

Table 2. Mean and standard deviation of O₃ 0-3km partial columns in Dobson Unit (DU) derived from raw and smoothed IAGOS, DIAL, and CAMS data, as well as IASI observations during the ACROSS campaign between June 13 to July 13 2022.

O ₃ column (0 - 3 km DU)								
	raw			N	smoothed			N
IAGOS	11.56	±	1.93	49	8.53	±	0.40	28
DIAL	12.88	±	2.38	52	8.55	±	0.49	42
CAMS	12.00	±	1.77	32	7.83	±	0.12	19
IASI AM	7.75	±	1.37	19				
IASI PM	6.25	±	0.98	19				
IASI	7.00	±	1.40	38				

Reference: Rodgers, C. D., and B. J. Connor (2003), Intercomparison of remote sounding instruments, *J. Geophys. Res.*, 108, 4116, doi:[10.1029/2002JD002299](https://doi.org/10.1029/2002JD002299), D3.

L305 – This statement regarding excellent agreement cannot be fully stated until the uncertainty estimations are presented or some level of description of the apriori data for IASI is described. References are critically needed throughout this section.

We agree with the referee and we have removed the comparison with the 1.2-3km O₃ partial columns in the revised manuscript. Instead, we have analyzed the sensitivity of the O₃ partial columns derived from IASI in terms of deviation from the a priori state, and Degrees Of Freedom for Signal (DOFS). Figure R2 (only included in this answer) shows that the O₃ 0-3 km partial columns and variabilities derived from IAGOS, DIAL and CAMS smoothed data are systematically lower than those calculated without taking into account the IASI averaging kernels. Smoothing with the IASI AKs reduces ozone columns and variability because part of the signal information comes from the *a priori* profile which is constant over time. However, IASI observations exhibit a variability of ~5 DU (mean of 7.00 ± 1.40 DU) over Paris during the ACROSS campaign, demonstrating that atmospheric signal is present in the retrieval information content with an averaged DOFS of 0.22 and 0.08 for morning and evening measurements, respectively.

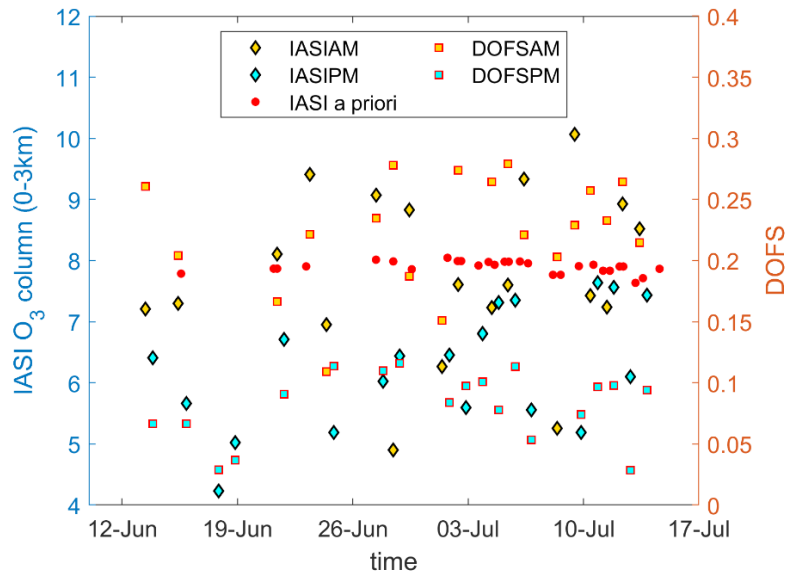


Figure R2: Timeseries of O₃ 0-3km partial columns of the retrievals (diamonds) and the a priori states (red dots), as well as Degrees Of Freedom for Signal (DOFS, squares) derived from IASI morning (yellow) and evening (cyan) observations.

Figure 13 – The IAGOS data does not replicate some of the higher ozone concentrations as observed in the DIAL measurements. What is the reason for this? This should also be labeled Partial Ozone columns in the x-axis.

The IAGOS profiles are only twice a day with the first profile in early morning at 4-6 UT and the second one either at 10 UT or at 14 UT. DIAL data are generally available each day for a longer time period 6 UT to 20 UT (see Fig. 5 and 6). The ozone maximum being observed in the afternoon it is not surprising to observe the largest variability with the DIAL data. The day-to-day variability is anyway still visible in the IAGOS data in Figure 8. As said earlier, the direct comparison between IAGOS, CAMS and DIAL vertical profiles is now better shown in the new section 3 (Fig. 7).

We have modified Figure 13 (new Figure 8) with the new y-label.

Section 5.2 - This could be better visualized by bringing at least one of the FLEXPART simulation plots to the main paper rather than the supplemental.

Done